Possible ergodic-nonergodic regions in the quantum Sherrington-Kirkpatrick spin glass model and quantum annealing

Sudip Mukherjee,[1,2,*] Atanu Rajak,[2,3,†] and Bikas K. Chakrabarti[2,‡]
[1]*Barasat Government College, Barasat, Kolkata 700124, India*
[2]*Condensed Matter Physics Division, Saha Institute of Nuclear Physics, 1/AF Bidhannagar, Kolkata 700064, India*
[3]*Department of Physics, Bar-Ilan University, Ramat-Gan 52900, Israel*

(Received 1 December 2017; published 28 February 2018)

We explore the behavior of the order parameter distribution of the quantum Sherrington-Kirkpatrick model in the spin glass phase using Monte Carlo technique for the effective Suzuki-Trotter Hamiltonian at finite temperatures and that at zero temperature obtained using the exact diagonalization method. Our numerical results indicate the existence of a low- but finite-temperature quantum-fluctuation-dominated ergodic region along with the classical fluctuation-dominated high-temperature nonergodic region in the spin glass phase of the model. In the ergodic region, the order parameter distribution gets narrower around the most probable value of the order parameter as the system size increases. In the other region, the Parisi order distribution function has nonvanishing value everywhere in the thermodynamic limit, indicating nonergodicity. We also show that the average annealing time for convergence (to a low-energy level of the model, within a small error range) becomes system size independent for annealing down through the (quantum-fluctuation-dominated) ergodic region. It becomes strongly system size dependent for annealing through the nonergodic region. Possible finite-size scaling-type behavior for the extent of the ergodic region is also addressed.

DOI: 10.1103/PhysRevE.97.022146

I. INTRODUCTION

A considerable number of investigations have studied the nonergodic behavior [1] of the spin glass phase of the classical Sherrington-Kirkpatrick (SK) spin-glass model [2]. The phenomenon of replica symmetry breaking, induced by nonergodicity, occurs due to the appearance of macroscopically high free-energy barriers separating the local minima. This highly rugged nature of the free-energy landscape in the spin glass phase causes the system to get trapped in any one (locally) self-similar region in the configuration space. Consequently one gets a broad order parameter distribution (or the replica symmetry breaking) in the spin glass phase as suggested by Parisi [3]. In this case, along with the peak at any nonzero value of the order parameter, its distribution also contains a long tail extending to the zero value of the order parameter in the thermodynamic limit. This localization due to nonergodicity has been determined to be responsible for the NP hardness of equivalent optimization problems (see, e.g., [4]).

The situation seems to be quite different when the SK spin glass is placed under a transverse field. Due to the presence of quantum fluctuations, the system is able to tunnel through the tall (but narrow) free-energy barriers [5–10], inducing ergodicity (or an absence of replica symmetry breaking). Consequently one would expect a narrowly peaked order parameter distribution in the quantum SK spin glass model in the thermodynamic limit [5]. This ergodicity has been identified to be responsible (see, e.g., [6] and [7]) for the success of quantum annealing.

We have studied the nature of the order parameter distribution of transverse-field SK spin glass at finite temperature using Monte Carlo simulation of the effective Suzuki-Trotter Hamiltonian and using the exact diagonalization technique at zero temperature. In this numerical study we tried to identify the possible ergodic spin glass phase (due to quantum tunneling) of the system. We find a low-temperature region in the quantum SK system, where the tails of the order parameter distribution vanish in the thermodynamic limit, suggesting the convergence of the order parameter distribution to be a peaked one around the most probable value. Although the system sizes we studied are not very large, we believe our study clearly indicates the existence of a low-temperature ergodic region in the spin glass phase of this quantum SK model. On the other hand, in the other (high-temperature) part of the spin glass phase, the order parameter distribution appears to remain the Parisi type [11], which indicates a lack of ergodicity in this part of the spin glass phase. We have already identified [12] the quantum-fluctuation-dominated part of the spin glass phase boundary of this model, crossing over at finite temperature to the classical-fluctuation-dominated part (see also [13]). Here we find that the line separating the ergodic and the nonergodic regions pass through the zero-temperature–zero-transverse-field point and the above-mentioned quantum-classical crossover point on the phase boundary.

We also study the variation of the average annealing time in the finite-temperature Suzuki-Trotter Hamiltonian dynamics for the model in both the ergodic and the nonergodic regions. For annealing down to a fixed low-temperature and low-transverse-field point through the (quantum-fluctuation-

*sudip.mukherjee@saha.ac.in
†raj.atanu009@gmail.com
‡bikask.chakrabarti@saha.ac.in

dominated) ergodic region, we find the average annealing time to be independent of the system size. On the other hand, the average annealing time is observed to grow strongly with the system size, when similar annealing is performed through the (classical-fluctuation-dominated) nonergodic region.

II. MODEL

The Hamiltonian of the quantum SK spin glass model with N Ising spins is given by (see, e.g., [7])

$$H = H_0 + H_I; H_0 = -\sum_{i<j} J_{ij}\sigma_i^z\sigma_j^z; H_I = -\Gamma\sum_{i=1}^{N}\sigma_i^x. \tag{1}$$

Here σ_i^z and σ_i^x are the z and x components of Pauli spin matrices, respectively, and Γ denotes the transverse field. The Hamiltonian in Eq. (1) becomes the classical SK spin glass Hamiltonian (H_0) for zero value of the transverse field. The spin-spin couplings (J_{ij}) follow a Gaussian distribution, $\rho(J_{ij}) = (\frac{N}{2\pi J^2})^{\frac{1}{2}} \exp(\frac{-NJ_{ij}^2}{2J})$, where the mean and standard deviation of the distribution are 0 and $J/\sqrt{N}$, respectively (see, e.g., [7]). In this work we take $J = 1$. To perform Monte Carlo simulation at a finite temperature we map Hamiltonian (1) into an effective classical Hamiltonian H_{eff} by using the Suzuki-Trotter formalism (see, e.g., [14]),

$$H_{\text{eff}} = -\sum_{m=1}^{M}\sum_{i<j}\frac{J_{ij}}{M}\sigma_i^m\sigma_j^m - \sum_{i=1}^{N}\sum_{m=1}^{M}\frac{1}{2\beta}\log\coth\frac{\beta\Gamma}{M}\sigma_i^m\sigma_i^{m+1}, \tag{2}$$

where σ_i^m ($=\pm1$) represents the ith (classical) Ising spin in the mth replica. We have an additional dimension [in Eq. (2)], namely, the Trotter dimension. Here M denotes the total number of Trotter slices and β is the inverse of the temperature T. $M \to \infty$ as $T \to 0$.

III. MONTE CARLO RESULTS

For the finite-temperature study, we perform a Monte Carlo simulation on H_{eff} to obtain the order parameter distribution in the spin glass phase of our model. To obtain this distribution function we first allow the system to equilibrate with t_0 Monte Carlo steps and the thermal averaging is done over the next t_1 time steps. In one Monte Carlo step we update all the spins of the system once. After the equilibration at each Monte Carlo step t we calculate the replica overlap $q^{\alpha\beta}(t)$, which is defined as $q^{\alpha\beta}(t) = \frac{1}{NM}\sum_{i=1}^{N}\sum_{m=1}^{M}(\sigma_i^m(t))^\alpha(\sigma_i^m(t))^\beta$. Here $(\sigma_i^m)^\alpha$ and $(\sigma_i^m)^\beta$ denote the spins of two replicas (in the mth Trotter slice) having identical sets of J_{ij}'s. The order parameter distribution $P(q)$ can be obtained as

$$P(q) = \overline{\frac{1}{t_1}\sum_{t=t_0}^{t_0+t_1}\delta(q - q^{\alpha\beta}(t))},$$

where the overbar denotes the configuration average over several sets of J_{ij}'s. The order parameter q is defined as $q = \frac{1}{MN}\sum_{m=1}^{M}\sum_{i=1}^{N}\overline{\langle\sigma_i^m\rangle^2}$, where $\langle\dots\rangle$ denotes the thermal average for a given configuration of disorder. From numerical data we compute the distribution function $P(q)$ for a given set of T and Γ by considering both area normalization and peak normalization (where the peaks of the distributions are normalized).

In our simulation we work with the system sizes $N = 60$, 120, 180, and 240, and the number of Trotter slices is $M = 15$. We have found that the equilibrium time of the system is not identical throughout the entire region of the Γ-T plane. The equilibrium time of the system (for $60 \leqslant N \leqslant 240$) is typically $\lesssim 10^6$ within the region $T < 0.25$ and $\Gamma < 0.40$, whereas it becomes $\lesssim 10^5$ for the rest of the spin-glass-phase region. We take $t_1 = 1.5 \times 10^5$ for Monte Carlo averaging and the configuration average is made over 1000 samples (configurations). Because of its symmetry we have determined the distribution of $|q|$ instead of q. We observe that the value of $P(|q|)$ for $q = 0$ has a clear system-size dependence. We extrapolate the values of $P(0)$ with $1/N$ to get the value of $P(0)$ for infinite system size. We also calculate the width W at half-maximum of the distribution function. The width W is defined as $W = |q_2 - q_1|$, where the value of $P(|q|)$ becomes half of its maximum value at $q = q_1, q_2$. Again, we extrapolate the values of W with $1/N$. We observe two distinct behaviors of such extrapolated values of both $P(0)$ and W in the spin glass phase. In the low-temperature (and high-transverse-field) case, we note that the values of $P(0)$ and W both go to 0 in the large-system-size limit [see Fig. 1(a)]. This observation indicates that $P(|q|)$ approaches Gaussian form in the thermodynamic limit, suggesting ergodic behavior of the system. In contrast, for the other case (high-temperature case) we find that $P(0)$ has a finite value even in the thermodynamic limit [see Fig. 1(b)]. There seems to be no possibility of $P(|q|)$'s approaching a Gaussian form of distribution for the infinite-system-size limit. This indicates that the system remains nonergodic in this region of the spin glass phase. To identify the ergodic and nonergodic regions in the spin glass phase more accurately, we also study the behavior of the peak-normalized order parameter distribution. From this study, again, we find that under a low temperature and high transverse field the values of $P(0)$ and W (extrapolated with $1/N$) become 0 in the thermodynamic limit [see Figs. 2(a) and 2(b)]. Again, from the peak-normalized order parameter distribution we find that for a high temperature and low transverse field the extrapolated values of the tail and width of distribution remain nonzero in the infinite-system-size limit [see Figs. 3(a) and 3(b)].

IV. ZERO-TEMPERATURE DIAGONALIZATION RESULTS

For the zero-temperature study with our model, we have investigated the distribution of the spin glass order parameter using an exact diagonalization technique. The diagonalization of the quantum spin glass has been performed using the Lanczos algorithm [15] to obtain its ground state. In this case we have considered system sizes (N) up to 20. The Hamiltonian in Eq. (1) can be written in spin basis states, which are indeed the eigenstates of the Hamiltonian H_0. After

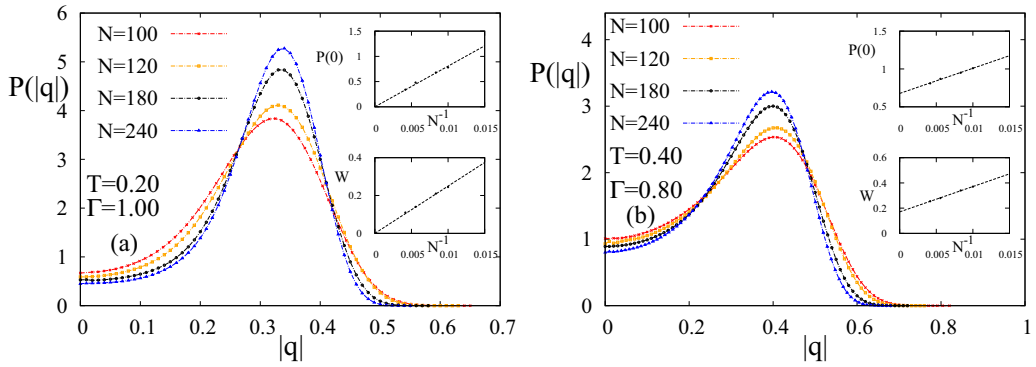

FIG. 1. Monte Carlo results for the plots of the area-normalized order parameter distribution $P(|q|)$ for given sets of transverse field Γ and temperature T values: (a) for $T = 0.20$ and $\Gamma = 1.00$; (b) for $T = 0.40$ and $\Gamma = 0.80$. Insets: Extrapolations of $P(0)$ with $1/N$. In the first case the extrapolated values of $P(0)$ and W tend to 0 in the large-system-size limit, whereas in the other case the values of such quantities remain finite even in the thermodynamic limit.

performing diagonalization, the nth eigenstate of the Hamiltonian in Eq. (1) is determined to be $|\psi_n\rangle = \sum_{\alpha=0}^{2^N-1} a_\alpha^n |\varphi_\alpha\rangle$, where $a_\alpha^n = \langle\varphi_\alpha|\psi_n\rangle$ and $|\varphi_\alpha\rangle$ denote the eigenstates of the Hamiltonian H_0. As a consequence of our interest in zero-temperature analysis, we focus here mainly on the ground-state ($|\psi_0\rangle$) averaging of different quantities of interest. One can define the order parameter for this zero-temperature system as $Q = (1/N)\sum_i \overline{\langle\psi_0|\sigma_i^z|\psi_0\rangle^2} = (1/N)\sum_i \overline{Q_i}$ (note that Q here for $T = 0$ differs from the q defined earlier for $T \neq 0$, using the replica average) [12]. Here, also, the overbar indicates configuration averaging. Q_i denotes the site-dependent local order parameter value. The distribution of the local order parameter is then represented by

$$P(|Q|) = \overline{\frac{1}{N}\sum_{i=1}^{N} \delta(|Q| - Q_i)}. \tag{3}$$

Similarly to the case of finite temperature, we here also have investigated the behavior of $P(|Q|)$ in the spin glass phase at different values of Γ. The variation of $P(|Q|)$ as a function of $|Q|$ at $\Gamma = 0.3$ is shown in Fig. 4 for four system sizes. It may be noted that in this case also we have plotted the distribution curves for different system sizes normalized to their maximum values as well as to the areas under the curves. In both the plots in Fig. 4, we observe that $P(|Q|)$ shows a peak at a finite value of $|Q|$ along with nonzero weight at $Q = 0$. However, the value of $P(0)$ decreases with an increase in the system size [although one can still detect an upward rise of $P(|Q|)$ for lower values of $|Q|$]. To get the behavior of $P(|Q|)$ in the thermodynamic limit, we have computed the value of $P(|Q|)$ for an infinite-size system for each $|Q|$ by plotting $P(|Q|)$ as a function of $1/N$. The extrapolation of $P(|Q|)$ for an infinite-size system is shown in both insets in Fig. 4, for $Q = 0.0$ and 0.1. In addition, we have also calculated the width (W) at half-maximum, $W = |Q_2 - Q_1|$, where at Q_2 and Q_1 the value of $P(|Q|)$ is half its maximum value. We plot W as a function of $1/N$ to get its extrapolated value for an infinite-size system (see Fig. 4). Finally, we have also plotted $P(|Q|)$ as a function of $|Q|$ with the extrapolated value of $P(|Q|)$ for infinite system size (see Fig. 4). One can observe that the $P(|Q|)$ curve for an infinite system becomes narrower compared to the cases of finite system size. On the other hand, due to the limitation of the maximum system size we could consider in our numerics, we are here not able to get a $P(|Q|)$ curve for very large system sizes showing results consistent with those derived from the delta function form. The effect of the limitation of the system size is also present in the plot of W with $1/N$ since the extrapolated W does not acquire a strictly

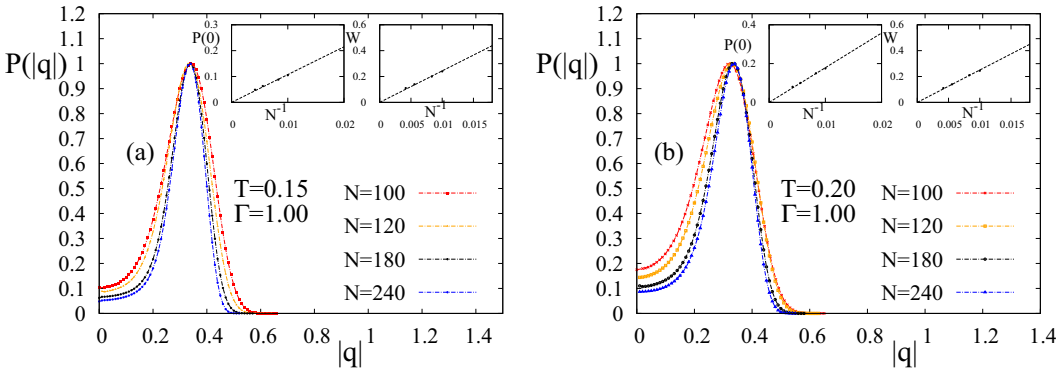

FIG. 2. Monte Carlo results for plots of the peak-normalized order parameter distribution $P(|q|)$ for given sets of transverse field Γ and temperature T values: (a) for $T = 0.15$ and $\Gamma = 1.00$; (b) for $T = 0.20$ and $\Gamma = 1.00$. Insets: Extrapolations of $P(0)$ with $1/N$. In both cases the extrapolated value of $P(0)$ tends to 0 in the large-system-size limit.

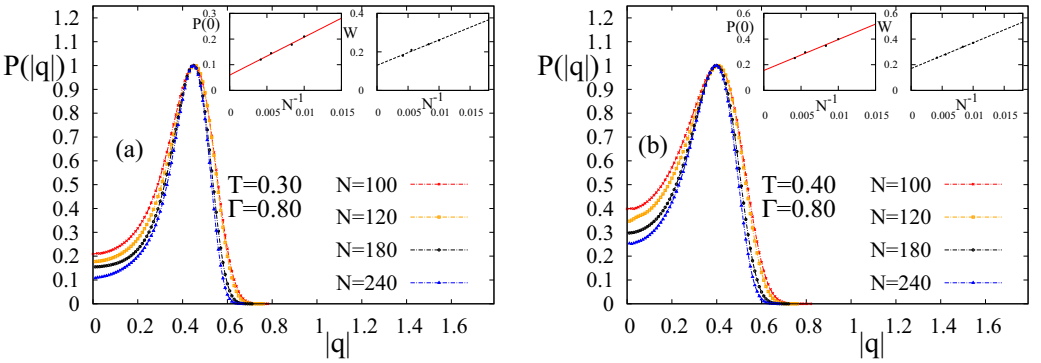

FIG. 3. Monte Carlo results for plots of the peak-normalized order parameter distribution $P(|q|)$ for given sets of transverse field Γ and temperature T values: (a) for $T = 0.30$ and $\Gamma = 0.80$; (b) for $T = 0.40$ and $\Gamma = 0.80$. Insets: Extrapolations of $P(0)$ with $1/N$. In these cases extrapolated values of $P(0)$ for the large-system-size limit remain finite.

zero value here. However, we infer from our extrapolated numerical analysis (from the results for small system sizes) that eventually the $P(|Q|)$ curve would become a delta function at finite values of $|Q|$ in the thermodynamic limit. This suggests that the system becomes ergodic in the spin glass phase at zero temperature with a definite spin glass order parameter value.

V. ANNEALING THROUGH ERGODIC AND NONERGODIC REGIONS

Our observations described in the earlier sections indicate clearly the existence of both ergodic (low-temperature and high-transverse-field) regions and nonergodic (high-temperature and low-transverse-field) regions, separated by a line originating from $T = 0$, $\Gamma = 0$ and the passing through the quantum-classical crossover point obtained earlier [12,13] on the phase boundary of the model. In order to check the dynamical features of these two regions, we have studied the annealing behavior of the system, again using the Suzuki-Trotter effective Hamiltonian with time (t)-dependent T and Γ: $T(t) = T_0(1 - \frac{t}{\tau})$ and $\Gamma(t) = \Gamma_0(1 - \frac{t}{\tau})$. Here T_0 and Γ_0 correspond to points in the para phase such that they are practically equidistant from the phase boundary line in different parts of the phase diagram. We look for the variation of the annealing time τ to reach a very low free energy (corresponding to very small values of $T \simeq 10^{-3} \simeq \Gamma$ to avoid singularities in the effective interaction H_{eff} and dynamics; putting these values of T and Γ into the last ($t = \tau$) step of the annealing schedule), starting from the para phase (high T and Γ values). We study annealing of the system when the annealing path (schedule) passes either through the ergodic or through the nonergodic region [see Fig. 5(a)]. We find that the annealing time τ remains fairly constant for any annealing path (schedule) passing entirely through the ergodic SG(E) region and becomes strongly system size (N) dependent as the path passes through the nonergodic region [see Fig. 5(b)]. It may be mentioned that, deep inside the classical region of the spin glass phase (for $S \gtrsim 1$; see Fig. 5), the annealing time becomes strongly configuration dependent and hence the N dependence of the average value of τ becomes somewhat irregular.

VI. DISCUSSION AND SUMMARY

We have studied the order parameter distribution in the spin glass phase of the quantum SK model, both at finite temperature [using Monte Carlo simulation of the effective Hamiltonian, (2)] and at zero temperature (using exact diagonalization). For Monte Carlo simulation we have taken system sizes $N = 60$,

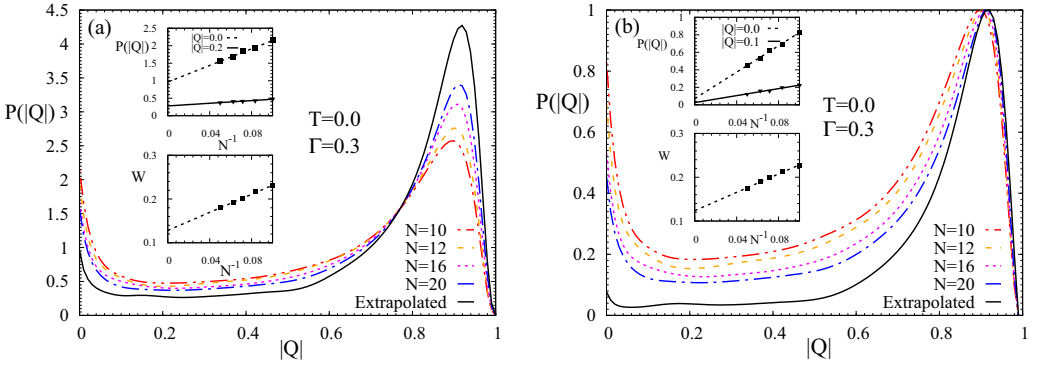

FIG. 4. Exact diagonalization results (at zero temperature) for the variation of $P(|Q|)$ as a function of $|Q|$ for quantum SK spin glass for four system sizes N at $T = 0$ and $\Gamma = 0.3$. (a) The area under the $P(|Q|)$ curves for each N is normalized to 1; (b) the peaks of all $P(|Q|)$ curves are normalized to their maximum values. In both plots, the extrapolated values of $P(|Q|)$ for large N (see insets) are plotted against $|Q|$ as well. Insets: Typical extrapolations of $P(|Q|)$, for $|Q| = 0.0$ and 0.1, and W with N.

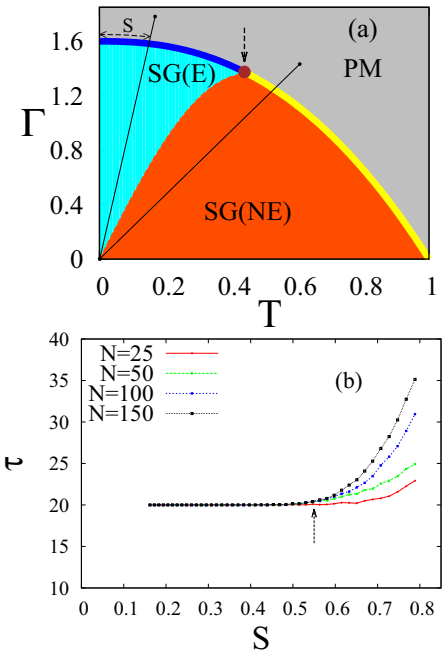

FIG. 5. (a) Schematic of the quantum SK model (cf. [12]). Here SG and PM denote the spin glass and paramagnetic phases, respectively. Our numerical simulations indicate that the spin glass phase is further divided into two regions: the ergodic SG(E) region and the nonergodic SG(NE) region. The filled red circle on the SG-PM phase boundary line indicates the quantum-classical crossover point in the critical behavior of the model [12,13]. We anneal by tuning both T and Γ following different linear paths passing through both SG(E) and SG(NE) regions (e.g., as indicated by the two diagonal straight lines). (b) Variation of annealing time τ with S, the length of the arc along the phase boundary starting from the pure quantum critical point ($T = 0$, $\Gamma \simeq 1.6$), up to the crossing point of the annealing line on the phase boundary. One does not get any system-size dependence of τ up to $S \simeq 0.55$ (corresponding to $T \simeq 0.46$, $\Gamma \simeq 1.35$; indicated in both panels by vertical arrows). As the annealing line passes through the SG(NE) region (beyond the quantum-classical crossover point), τ is seen to acquire a strong system-size dependence.

120, 180, and 240 along with Trotter size $M = 15$ (Figs. 2 and 3). It may be mentioned that we checked that the Monte Carlo results remain practically unchanged if for such system sizes we vary the number of Trotter slices M with the system size N, keeping the value of the scaled variable $M/N^{z/d}$ constant, where z denotes the dynamical exponent and d is the effective dimension of the system (see [12] for details). For zero-temperature analysis we considered the system sizes $N = 10$, 12, 16, and 20 (Fig. 4). In the ergodic region SG(E) [see Fig. 5(a)], the (extrapolated) order parameter distribution is found to converge to a Gaussian form around the most probable value with increasing system size [see Figs. 2(a) and 2(b) for $T \neq 0$]. Although at $T = 0$ the system sizes we considered are very small, it can be anticipated that we will get a single and narrow peak in the order parameter distribution (see Fig. 4) around the most probable value for thermodynamically large systems, indicating the ergodicity of the spin glass phase at zero temperature. On the other hand, in the nonergodic region SG(NE) [see Fig. 5(a)], we get a Parisi-type order parameter distribution where the long tail extends up to zero value of the order parameter [see Figs. 3(a) and 3(b)]. This (nonzero) weight of the distribution near the origin remains nonvanishing with increasing system size N. This behavior of the order parameter distribution indicates the absence of ergodicity in the system in the SG(NE) region.

These results indicate the different regions of the spin glass phase of the quantum SK model as shown in Fig. 5(a). It may be noted that the line separating the low-temperature (quantum-fluctuation-driven) ergodic region of the quantum spin glass phase from the high-temperature nonergodic region passes through the quantum-classical crossover point on the spin glass phase boundary obtained earlier [12,13]. Apart from this low-temperature part of the spin glass phase the entire para phase of course remains ergodic.

In order to test the role of this quantum-fluctuation-induced ergodicity in the spin glass phase here, we have also studied the variation of the annealing time τ in finite-temperature Suzuki-Trotter Hamiltonian dynamics for $T(t) = T_0(1 - \frac{t}{\tau})$ and $\Gamma(t) = \Gamma_0(1 - \frac{t}{\tau})$ to reach a desired low value of the free energy (corresponding to very low, but finite, values of T and Γ, to avoid singularities in the effective interaction flipping dynamics). Here T_0 and Γ_0 values of course correspond to the para phase. For such annealing through the ergodic region we have found τ to be fairly independent of the system size N. However, it clearly starts growing with N as one enters the nonergodic region [see Fig. 5(b)].

We believe the numerical results reported here for the quantum SK model establish the nature of the earlier conjectured [5] ergodicity in the model and its role in quantum annealing [6,7,16] of the SK model. It is also possible that the crossover region shrinks as $N \to \infty$. Indeed there are several publications [17–19] which contradict our conjecture and suggest these results to be due to finite-size effects in the numerical simulations (of course, the paper by Read *et al.* suggests ergodicity or absence of replica symmetry breaking as $T \to 0$). The same criticisms are also applied in [19] to the experimental and numerical observations [13] for "scrambling" or ergodicity in this system at low enough temperatures. Even if these effects are due to a finite system size and the ergodic region becomes narrower with increasing system size, it is important to study such "finite-size-scaling"-like behavior of the annealing dynamics, so that one can perhaps extrapolate properly the finite-size annealing results as the system size approaches the macroscopic limit. Such an extrapolation scheme, if formulated properly, will be extremely useful for quantum annealing machines (like the D-wave [20]) already developed and for developing the quantum machine learning algorithms [21].

ACKNOWLEDGMENTS

We are grateful to Arnab Chatterjee, Arnab Das, Sabyasachi Nag, Purusattam Ray, and Parongama Sen for their comments and suggestions. Bikas Chakrabarti gratefully acknowledges his J. C. Bose Fellowship (DST) Grant. A.R. acknowledges financial support from the Israeli Science Foundation Grant No. 1542/14.

[1] K. Binder and A. P. Young, Rev. Mod. Phys. **58**, 801 (1986).
[2] D. Sherrington and S. Kirkpatrick, Phys. Rev. Lett. **35**, 1792 (1975).
[3] G. Parisi, J. Phys. A **13**, L115 (1980).
[4] A. Das and B. K. Chakrabarti, Rev. Mod. Phys. **80**, 1061 (2008).
[5] P. Ray, B. K. Chakrabarti, and A. Chakrabarti, Phys. Rev. B. **39**, 11828 (1989).
[6] S. Mukherjee and B. K. Chakrabarti, Eur. Phys. J. Special Topics **224**, 17 (2015).
[7] S. Tanaka, R. Tamura, and B. K. Chakrabarti, *Quantum Spin Glasses, Annealing and Computation* (Cambridge University Press, Cambridge, UK, 2017).
[8] S. Mandra, Z. Zhu, and H. G. Katzgraber, Phys. Rev. Lett. **118**, 070502 (2017).
[9] T. Albash and D. Lidar, Rev. Mod. Phys. **90**, 015002 (2018).
[10] D. Herr, E. Brown, B. Heim, M. Könz, G. Mazzola, and M. Troyer, arXiv:1705.00420.
[11] A. P. Young, Phys. Rev. Lett. **51**, 1206 (1983).
[12] S. Mukherjee, A. Rajak, and B. K. Chakrabarti, Phys. Rev. E **92**, 042107 (2015).
[13] N. Y. Yao, F. Grusdt, B. Swingle, M. D. Lukin, D. M. Stamper-Kurn, J. E. Moore, and E. Demler, arXiv:1607.01801.
[14] A. Dutta, G. Aeppli, B. K. Chakrabarti, U. Divakaran, T. Rosenbaum, and D. Sen, *Quantum Phase Transitions in Transverse Field Models* (Cambridge University Press, Cambridge, UK, 2015).
[15] A. W. Sandvik, AIP Conf. Proc. **1297**, 135 (2010).
[16] A. Rajak and B. K. Chakrabarti, Ind. J. Phys. **88**, 951 (2014).
[17] Y. Goldschmidt and P.-Y. Lai, Phys. Rev. Lett. **64**, 2467 (1990).
[18] N. Read, S. Sachdev, and J. Ye, Phys. Rev. B. **52**, 384 (1995).
[19] A. P. Young, Phys. Rev. E. **96**, 032112 (2017).
[20] V. S. Denchev, S. Boixo, S. V. Isakov, N. Ding, R. Babbush, V. Smelyanskiy, J. Martinis, and H. Neven, Phys. Rev. X **6**, 031015 (2016).
[21] C. Baldassi and R. Zecchina, Proc. Natl. Acad. Sci. USA **115**, 1457 (2018).